Bone-suppressed radiography using machine learning

Junbeom Park [a], Daecheon Kim [a], Ho Kyung Kim [a,b*]
[a]*School of Mechanical Engineering, Pusan National University Busan 46241, South Korea*
[b]*Center for Advanced Medical Engineering, Pusan National University, Busan 46241, South Korea*
[*]*Corresponding author: Hokyung@pusan.ac.kr*

1. Introduction

Digital radiography projects a three-dimensional object into a two-dimensional plane. Therefore, lesions can be hidden by normal tissues or the superimposed normal tissues can be sometimes misunderstood as lesions. To enhance lesion conspicuity in digital radiography by removing or reducing the background clutter, many researches have been conducted: dual-shot dual-energy imaging [1] single-shot dual-energy imaging [2,3] and digital chest tomosynthesis [4]. Each development has its own disadvantages. For example, the double-shot dual-energy imaging is susceptible to the motion artifacts because of the time interval between two successive exposures [5]. The single-shot dual-energy imaging suffers from reduced contrast-to-noise ratio performance due to poor spectral separation [2,3,6]. Tomosynthesis requires more complex motion equipment and may require higher patient dose.

An alternative tissue-specific imaging technique was introduced [7,8,9]. This alternative technique usually possesses a filter to generate bone-only images for given digital radiographs. Therefore, it provides soft-tissue-enhanced images from the subtraction of given radiographs and filtered bone-only images. Only bone-suppressed imaging capability is a limitation of the method. The filter can be obtained from a machine-learning algorithm, e.g. artificial neural network (ANN), with the dual-energy bone-only images (called 'teaching' images). We suspect the robustness of the filter may be dependent upon the number of teaching images and the number of patients from whose radiographs we obtain the teaching images.

In this study, we design an ANN to obtain a bone-extracting filter from a radiograph, and investigate the filter properties with respect to various ANN parameters.

2. Materials and Methods

The ANN can be regarded as an interconnected group of units. Fig. 1. shows a graphical model of ANN considered in this study. It mainly consists of three layers: input, hidden, and output layers. Each layer consists of N, M, and L units, respectively. Actually, the input and hidden layer respectively require one additional unit as bias (see below). Each unit represents an artificial neuron and lines represent connections (i.e. weights) from the output of one neuron to the input of another. In general, the output of a neuron is determined (or activated) by an activation function:

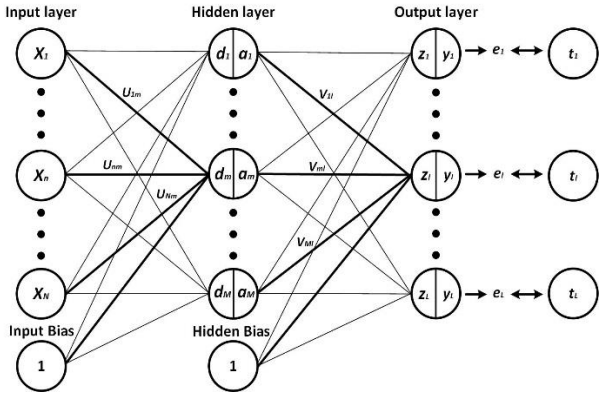

Fig. 1. A simple artificial neural network considered in this study. It consists of the input, hidden, and output layers, which of each includes N+1, M+1, and L units, respectively.

$$\varphi(\chi, \omega) = f(\textstyle\sum_j \omega_j \phi_j(\chi)) \qquad (1)$$

where χ = the input signal vector, ω = the weight, $\phi(\chi)$ = fixed non-linear basis functions, and f = the activation function.

For training the network, the final output signal is first calculated through the forward direction using the relationship, as shown in Eq. (1), and the calculated output signal is compared with the given teaching signal. Then, the weights are modified to reduce the difference between the output and teaching signals. For example, the amount of change in weights is determined by differentiating the error (i.e. the difference) with respect to weights, and which is known as the gradient descent method. This sequential process is repeated until it converges. The update of weight matrix at the present state, $W^{(i)}$, can be described with the weight matrix $W^{(i-1)}$ and the error $\epsilon^{(i-1)}$ obtained at the previous state:

$$W^{(i)} \leftarrow W^{(\mathrm{i}-1)} - \eta \frac{\partial \epsilon^{(i-1)}}{\partial W^{(i-1)}} \qquad (2)$$

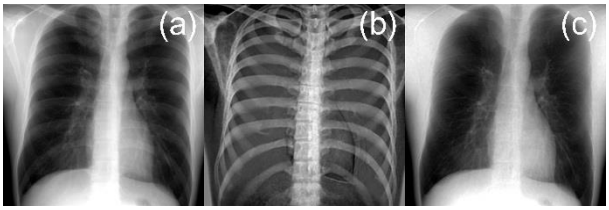

Fig. 2. Dual-energy images obtained from a commercial fast kVp-switching system: (a) high-energy (120 kVp) image, (b) bone-enhanced image, and (c) tissue-enhanced image.

where η is called the learning rate and it affects the convergence speed. Since the weights are modified from the output side to input side, this process is called the error backpropagation.

For training the network, dual-energy images were obtained for a patient using a commercial system (Definium 8000, GE Healthcare, US) as shown in Fig. 2. In this preliminary study, the images were re-sized to small versions (400 × 400 pixel format) for a computational efficiency. The trained network performance was evaluated by calculating structural similarity index (SSIM) [10] between the soft tissue image obtained using the network and the ground-truth image obtained from the commercial equipment.

3. Preliminary result

Preliminary results are summarized in Fig. 3. We extracted 5,000 subregions in a 21×21 pixel format from the lung region in the bone-enhanced dual-energy image and we used them for teaching images during training the ANN. The resultant bone-enhanced image from the ANN nonlinear filter is shown in Fig. 3 (a). From the weighted logarithmic subtraction between Fig. 2 (a) and Fig. 3 (a), we could obtain the bone-suppressed image as shown in Fig. 3 (b). The quality of the bone-suppressed image is comparable to the ground truth Fig. 2 (c).

4. Further Study

As shown above, the ANN bone-suppressed imaging is promising. The question is that the ANN filter determined from a single patient can be universally applied to any patient radiographs. The remained further study before the meeting includes the followings.

First, investigation of the general properties of ANN nonlinear filters in terms of various parameters such as the size of teaching image, the learning rate, the number of layers and units, and so on.

Second, investigation of the robustness of ANN filters with respect to the number of patient data.

To achieve the purpose of this study, the development of quantitative numerical and experimental models is in progress.

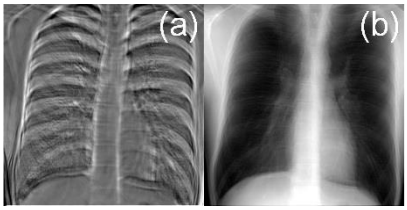

Fig. 3. (a) Bone-enhanced image using the ANN nonlinear filter, (b) bone-suppressed image by applying (a) to chest radiograph.

ACKNOWLEDGMENTS

This work was supported by the National Research Foundation of Korea (NRF) grant funded by the Korea government (MSIP) (No. 2013M2A2A9046313, No. 2014R1A2A2A01004416).

REFERENCES

[1] H. Kashani, C. A. Varon, N. S. Paul, G. J. Gang, R. V. Metter, J. Yorkston, and J. H. Siewerdsen, Diagnostic performance of a prototype dual-energy chest imaging system: ROC analysis, Acad. Radiol., Vol. 17(3), pp.298-308, 2010.

[2] R. E. Alvarez, J. A. Seibert, and S. K. Thompson, Comparison of dual energy detector system performance, Med. Phys., Vol. 31(3), pp. 556–565, 2004.

[3] J. C. Han, H. K. Kim, D. W. Kim, S. Yun, H. Youn, S. Kam, J. Tanguay, and I. A. Cunningham, Singleshot dual-energy x-ray imaging with a flat-panel sandwich detector for preclinical imaging, Cur. Appl. Phys., Vol. 14(12), pp. 1734–1742, 2014.

[4] J. T. Dobbins III and H. P. McAdams, Chest tomosynthesis: Technical principles and clinical update, Eur. J. Radiol. Vol. 72(2), pp. 244–251, 2009.

[5] N. A. Shkumat, J. H. Siewerdsen, A. C. Dhanantwari, D. B. Williams, N. S. Paul, J. Yorkston, and R. V. Metter, Cardiac gating with a pulse oximeter for dual-energy imaging, Phys. Med. Biol., Vol. 53(21), pp. 6097–6112, 2008.

[6] S. Richard and J. H. Siewerdsen, Optimization of dual-energy imaging systems using generalized NEQ and imaging task, Med. Phys., Vol. 34(1), pp. 127–139, 2007.

[7] F. Li, T. Hara, J. Shiraishi, R. Engelmann, H. MacMahon, and K. Doi, Improved detection of subtle lung nodules by use of chest radiographs with bone suppression imaging: Receiver operating characteristic analysis with and without localization, Am. J. Roentgenol., Vol. 196, pp. W535–W541, 2011.

[8] J.-S. Lee, J.-W. Wang, H.-H. Wu, and M.-Z. Yuan, A nonparametric-based rib suppression method for chest radiographs, Comput. Math. Appl., Vol. 64(5), pp. 1390–1399, 2012.

[9] S. Chen and K. Suzuki, Separation of bones from chest radiographs by means of anatomically specific multiple massive-training ANNs combined with total variation minimization smoothing, IEEE Trans. Med., Imaging 33, pp. 246–257, 2014.

[10] Z. Wang, A. Bovik, H. Sheikh, and E. Simoncelli, Image quality assessment: From error visibility to structural similarity, IEEE Trans., Image Process 13, pp. 600–612, 2004.